The Astrophysical Journal, 663:L57–L60, 2007 July 10

PROPERTIES OF A GAMMA-RAY BURST HOST GALAXY AT $z \sim 5$[1]

P. A. Price,[2] A. Songaila,[2] L. L. Cowie,[2] J. Bell Burnell,[3] E. Berger,[4] A. Cucchiara,[5] D. B. Fox,[5] I. Hook,[3] S. R. Kulkarni,[6] B. Penprase,[7] K. C. Roth,[8] and B. Schmidt[9]

Received 2007 March 29; accepted 2007 May 22; published 2007 June 18

ABSTRACT

We describe the properties of the host galaxy of the gamma-ray burst GRB 060510B based on a spectrum of the burst afterglow obtained with the Gemini North 8 m telescope. The galaxy lies at a redshift of $z = 4.941$, making it the fourth highest spectroscopically identified burst host. However, it is the second highest redshift galaxy for which the quality of the spectrum permits a detailed metallicity analysis. The neutral hydrogen column density has a logarithmic value of 21.0–21.2 cm^{-2}, and the weak metal lines of Ni, S, and Fe show that the metallicity is in excess of a tenth of solar, which is far above the metallicities in damped Lyα absorbers at high redshift. The tightest constraint is from the Fe lines, which place [Fe/H] in excess of -0.8. We argue that the results suggest that metallicity bias could be a serious obstacle to inferring star formation from the GRB population, and we consider how future higher quality measurements could be used to resolve this issue.

Subject headings: cosmology: observations — galaxies: abundances — galaxies: distances and redshifts — galaxies: evolution — gamma rays: bursts

1. INTRODUCTION

Long-duration gamma-ray bursts (GRBs) are believed to form during the collapse of massive stars (e.g., Woosley 1993; Stanek et al. 2003), and hence they become tracers of galaxies with ongoing star formation (Lamb & Reichart 2000). The afterglows associated with a burst are also extremely bright immediately postburst and can be seen to very large redshifts, currently out to $z = 6.2$ (Kawai et al. 2006). Prompt spectroscopy of the afterglow can therefore allow us to obtain the redshift of the galaxy in which the GRB has occurred and to study the metallicity of the interstellar medium in this host galaxy.

With the caveat that we still do not fully understand the selection biases introduced by the formation of the GRBs, this may be the best way in which we can study the properties of individual galaxies at very high redshifts ($z > 5$) in detail. The galaxies themselves are too faint (magnitudes of about 25) for detailed spectroscopic study, nor can they be identified as damped Lα absorbers (DLAs) at these redshifts since the Lα forest becomes too thick to allow us to identify the DLAs and measure their column densities.

However, in order to take advantage of GRBs to study the high-redshift galaxy population, we must be able both to localize the GRB quickly and then to rapidly identify it as a candidate high-redshift object. The *Swift* satellite launched in 2004 (Gehrels et al. 2004) has made such studies possible by providing a large sample of GRBs with accurate positions to faint gamma-ray detection thresholds. At the *Swift* limits, Jakobsson et al. (2006a) estimate that about 7% of the GRBs are at $z > 5$, so that there should be a handful of such objects available for study in each year of the *Swift* mission.

Given this small number of available targets, it is critical to observe as many as possible with the highest quality and highest resolution spectroscopy that we can obtain. However, even with the *Swift* data, this remains extremely challenging since we must first identify the afterglow and since the subsequent spectroscopy requires target of opportunity (ToO) observations on the largest ground-based telescopes. Fortunately, some of the 8 m–class telescopes are operated in queue mode and can respond rapidly to such ToO events. The present program utilizes this capability on the two Gemini 8 m telescopes where we can initiate observations with the Gemini Multi-Object Spectrograph (GMOS; Hook et al. 2004) almost immediately when a candidate high-redshift burst is identified. The GMOS spectral resolution ($R \sim 2000$ in the mode that we used) is not as high as desirable but is adequate for measuring the redshift and providing metallicity estimates if we can obtain high signal-to-noise ratio spectra.

This Letter describes our GMOS observations of GRB 605010B, which we find to lie at a redshift of $z = 4.941$. This is the fourth highest redshift identified for a GRB (see, e.g., Jakobsson et al. 2006b for a recent summary) but is the second highest for which we can make a metallicity analysis. The highest redshift analysis is of the $z = 6.2$ GRB (Kawai et al. 2006). We find that the metallicity is in excess of a tenth solar, which is much higher than is seen in DLAs at $z > 4$ and also suggests that the metallicity of the GRB host galaxies is not changing as a function of redshift.

2. OBSERVATIONS

GRB 060510B was detected by *Swift* on 2006 May 10 at 8:22:24 UT. The X-ray Telescope on *Swift* began observing the area 119 s after the trigger, and a bright X-ray source was

[1] Based on observations obtained at the Gemini Observatory, which is operated by the Association of Universities for Research in Astronomy, Inc., under a cooperative agreement with the NSF on behalf of the Gemini Partnership: the National Science Foundation (US), the Particle Physics and Astronomy Research Council (UK), the National Research Council (Canada), CONICYT (Chile), the Australian Research Council (Australia), CNPq (Brazil), and CONICET (Argentina)

[2] Institute for Astronomy, University of Hawaii, 2680 Woodlawn Drive, Honolulu, HI 96822.

[3] Astrophysics, University of Oxford, Denys Wilkinson Building, Keble Road, Oxford OX1 3RH, UK.

[4] Observatories of the Carnegie Institution of Washington, 813 Santa Barbara Street, Pasadena, CA 91101

[5] Department of Astronomy and Astrophysics, Pennsylvania State University, 525 Davey Laboratory, University Park, PA 16802.

[6] Mail Code 105-24, Astronomy, California Institute of Technology, 1200 East California Boulevard, Pasadena, CA 91125.

[7] Pomona College, 610 North College Avenue, Claremont, CA 91711.

[8] Gemini Observatory, 670 North A'ohoku Street, Hilo, HI 96720.

[9] Research School of Astronomy and Astrophysics, Australian National University, Mount Stromlo Observatory, Cotter Road, Weston Creek, Canberra, ACT 2611, Australia.

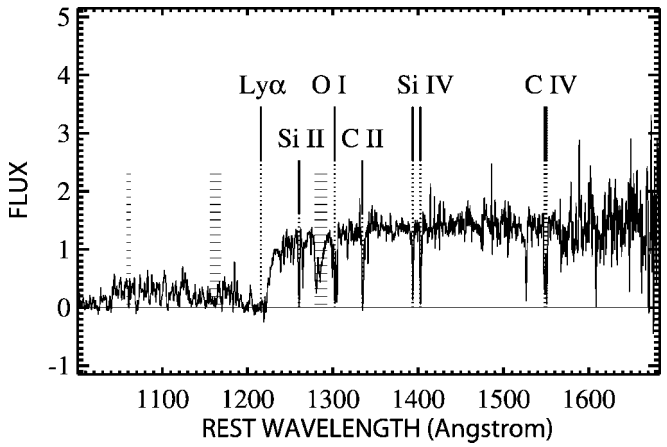

FIG. 1.—Spectrum of GRB 060510B obtained with the 400 line mm^{-1} grating on the GMOS on Gemini. We have made an approximately relative flux calibration of the spectrum based on the instrument throughput but have not attempted an absolute flux calibration. The exposure time was 2000 s. The spectrum is shown in the rest frame of the host galaxy at a redshift $z = 4.941$, and the strong lines of Lα, Si II, O I, C II, Si IV, and C IV are marked. The horizontal bars show the positions of the atmospheric bands and strong night-sky lines.

located at R.A. = $15^h56^m29.3^s$, decl. = 78°34′09.4″ (J2000). The long-duration gamma-ray burst was noted as a potential high-redshift object (Krimm et al. 2006). A fading optical counterpart was detected by Mirabal & Halpern (2006) at R.A. = $15^h56^m29.615^s$, decl. = 78°34′13.02″. The red ($R - I$) color was again suggestive of a possible high-redshift candidate. Near-IR Imager observations with Gemini North detected the counterpart with $J \sim 19$ at just over 2 hr after the trigger (Price et al. 2006b).

We obtained a spectrum with the GMOS on Gemini North, commencing at 2006 May 10.547 UTC just over 2.5 hr after the burst (Price et al. 2006c). Four 1000 s exposures were obtained with the 400 line mm^{-1} grating, giving a resolution of 1900 and wavelength coverage from 5950 to 10200 Å. Standard CCD reduction steps were performed with the `gmos` package within IRAF, pairs of exposures were sky-subtracted and combined, the spectra extracted using `apextract`, and the two spectra summed to yield the final product. The spectrum was approximately relatively flux-calibrated using the instrument throughput. The final spectrum is shown in Figure 1.

The spectrum shows a damped Lα line and an extensive set of metal lines at a redshift of $z = 4.941$, which we take to be the redshift of the host galaxy. Some of the stronger features in the spectrum are marked in Figure 1. The spectrum also shows a strong break across the Lα wavelength corresponding to the onset of the Lα forest at shorter wavelengths. The mean transmission in the Lα forest is 18%, consistent with Lα forest transmissions seen in quasar spectra at this redshift (Songaila 2004).

3. HOST PROPERTIES

We first measured a redshift of $z = 4.941$ from the weaker singly ionized metal lines in the spectrum. Fits to the damped Lα and Lβ lines centered at the wavelength corresponding to this redshift are shown in Figure 2. The best fit to the red wing of the damped Lα profile is given for a N(H I) = 1.7×10^{21} cm^{-2}, and higher column densities are prohibited. The Lβ profile favors a slightly lower value of N(H I) = 1.0×10^{21} cm^{-2}, but this constraint is based on a single pixel that could be contaminated.

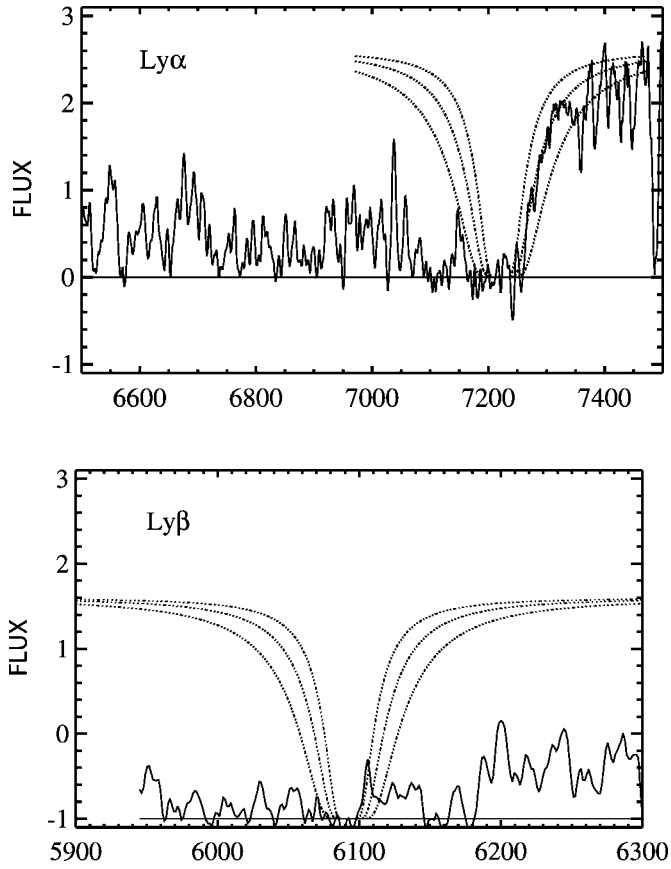

FIG. 2.—Damped Lα and Lβ profiles for N(H I) of 1×10^{21}, 2×10^{21}, and 4×10^{21} cm^{-2}.

We therefore adopt a range of log N(H I) = 21.0–21.2 for the logarithmic column density.

A second strong absorption feature seen in the Lα forest at 7100 Å is not saturated at Lβ and is not a DLA. This neutral hydrogen excess may be caused by the higher density intergalactic medium in the vicinity of the galaxy, and it will be interesting to see if this is common in GRBs at these redshifts since it could provide considerable information on the structure and ionization of the overdense regions in which the galaxies are forming.

Although we detect many lines from the galaxy, most are strong and, in low-resolution spectra like the present one, the lower limits on the column densities that can be obtained from such lines are not particularly useful. We therefore focus on the weaker lines of Ni, S, and Fe that are seen in the spectrum. The absorption profiles of some of these lines are shown in Figure 3.

Even in these moderately weak lines, saturation can be a problem, and saturated components can be masked by unsaturated features in the lines. This problem, long familiar in interstellar medium studies, has recently been reemphasized in Prochaska (2006), where an extensive discussion and critique of GRB host metallicity measurements can be found, as well as the many historical references on the topic. For the present work, we measured the various Ni, S, and Fe lines under the assumption that they are unsaturated and lie in the strictly linear portion of the curve of growth. The column densities measured in this way and their 1 σ uncertainties are given in Table 1. We emphasize that these are only lower limits to the column density. If there are narrow saturated components concealed in

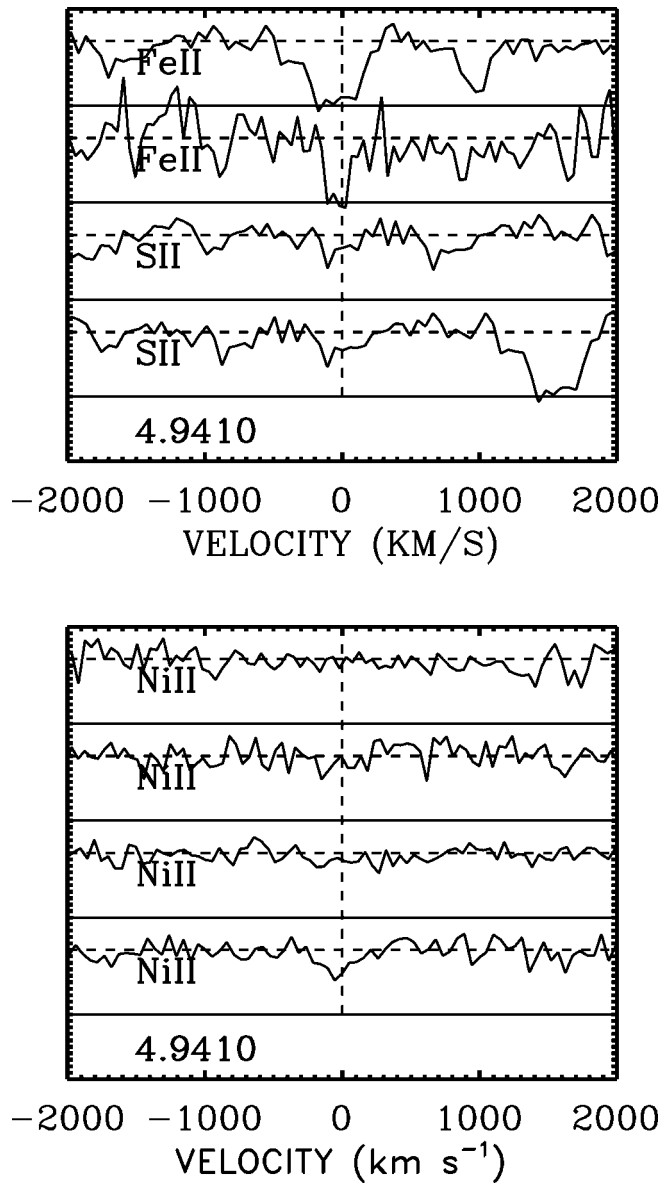

FIG. 3.—*Upper panel, bottom to top*: Lines S II λ1251, S II λ1254, Fe II λ1608, and Fe II λ1260. *Lower panel, bottom to top*: Lines Ni II λ1317, Ni II λ1370, Ni II λ1455, and Ni II λ1467. For each species, the lines are shown in order of decreasing oscillator strength, with the stronger lines at the bottom and the weaker at the top. The higher noise at Fe 1608 Å is a result of decreasing throughput at longer wavelengths.

TABLE 1
COLUMN DENSITIES

Ion	λ (Å)	f	log N (cm^{-2})
H I	1215.67	0.416	21.1 ± 0.1
Fe II	1608.45	0.062	>15.9
S II	1250.58	0.005	15.6 (14.8–15.9)
	1253.81	0.011	15.5 ± 0.2
Ni II	1317.22	0.145	14.4 ± 0.2
	1370.13	0.131	14.0 ± 0.2
	1454.84	0.0595	14.4 (14.0–14.6)

NOTE.—All errors are 1 σ.

TABLE 2
METALLICITIES

Element	Solar	Relative
S	−4.86	−0.8 ± 0.3
Fe	−4.55	−0.3 to −0.8
Ni	−5.77	−1.2 ± 0.3

the absorption lines, the column density could be higher. However, even these lower limits already place a lower limit on the metallicity of about −1 relative to solar (Asplund et al. 2005; Table 2), which is already considerably higher than the values seen in DLAs at $z > 4$ (Prochaska et al. 2003). We illustrate this in Figure 4.

If the signal-to-noise ratio is high enough, we can use very weak lines to measure upper bounds on the metallicity, even in low-resolution spectra (e.g., Savaglio 2006). However, the quality of the very high redshift GRB spectra is not generally adequate to do this. We tested the limits that we could obtain in the present data using the very weak Fe λ1611 and Ni λ1467 lines. In each case, we created a model with two components each with $b = 8$ km s^{-1} and two broader ($b = 50$ km s^{-1}) components, and adjusted the column densities to fit the stronger lines (here b is 0.60 times the full width at half-maximum of the absorption line; Cowie & Songaila 1986). We varied the column densities in the narrow components and compared the resulting Voigt profiles with the weak lines. Within the noise and continuum fitting uncertainties, we cannot obtain a robust upper limit on the column densities.

The spectrum also shows strong high-ionization lines with log N(N V) in excess of 14.5 and log N(C IV) and log N(Si IV) in excess of 15. Strong fine-structure lines are seen for Si II, C II, and O I, as is common to all the GRB absorbers (Vreeswijk et al. 2004; Berger et al. 2006; Chen et al. 2005). Given the uncertainty in estimating the ground-state column densities, we do not attempt

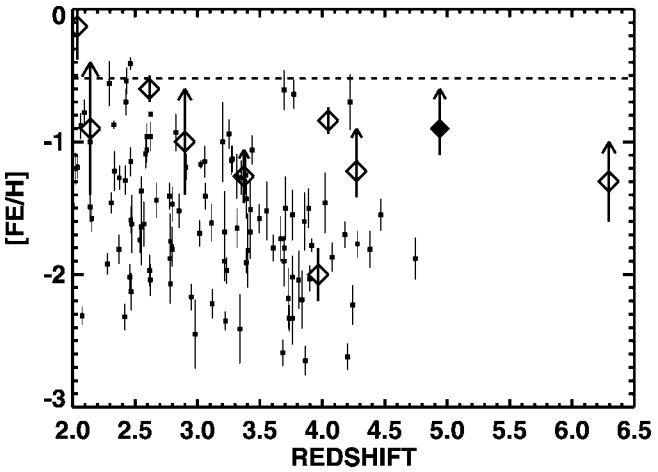

FIG. 4.—Metallicity relative to solar vs. redshift for the GRB host galaxies (*diamonds*) superimposed on the corresponding measurements of metallicity in damped Lyα systems along quasar sight lines, taken from the compilation of Prochaska et al. (2003). The value measured in this Letter is shown as the filled diamond and is based on the S II, Fe II, and Ni II measurements of Table 2. The open diamonds show values from the literature (Savaglio et al. 2003; Vreeswijk et al. 2004, 2006; Chen et al. 2005; Starling et al. 2005; Watson et al. 2006; Berger et al. 2006; Fynbo et al. 2006; Ledoux et al. 2005; Kawai et al. 2006). For lower resolution measurements (including the present measurement) where saturation effects could significantly raise the measured metallicity, we plot the data with an upward-pointing arrow. The dashed line shows the metallicity above which GRBs are not expected to form in collapsar models.

to infer gas densities, but it is clear, as has been noted by many authors, that GRB absorption is produced in much higher gas density environments than DLAs in quasar sight lines, which only extremely rarely show such lines (e.g., Chen et al. 2005).

4. DISCUSSION

In Figure 4 we show all of the currently available metallicity measurements for $z > 2$ GRB host galaxies from the references summarized in the figure caption. The present measurement of GRB 0605010B is shown as the filled diamond with upward-pointing arrow to emphasize that it is strictly a lower limit. We show the other measurements of the GRB hosts as open diamonds. We show measurements based on low-resolution and moderate signal-to-noise ratio spectra with upward-pointing arrows on 1 σ error bars, while values based on high-resolution or high signal-to-noise ratio observations are shown with just the 1 σ errors. Irrespective of redshift, the bulk of the GRB metallicities reported so far lie at or above about a tenth solar. However, GRB hosts clearly have a wide range of metallicities; for example, compare GRB 050730 ($z = 3.969$; Chen et al. 2005) with a metallicity of -2 and GRB 000926 ($z = 2.038$; Savaglio et al. 2003) with a metallicity of -0.13.

The typical metallicity of GRB host galaxies is considerably higher than the metallicities found in DLAs, which are shown in Figure 4 as the filled squares. However, there is only one $z > 4.5$ DLA with a measured metallicity (Songaila & Cowie 2002), so the comparison sample at the highest redshifts is very limited. This effect and the higher gas densities evidenced by the fine-structure lines are natural consequences of the selection biases. GRB sight lines target star-forming regions of galaxies where densities and metallicities will be higher, whereas the cross section–weighted DLAs in quasar sight lines probe more extended lower density and lower metallicity regions in galaxies and may also be weighted to intrinsically lower luminosity galaxies.

Ultimately, we would like to use GRBs to probe the star formation history of the universe (Lamb & Reichart 2000; Price et al. 2006a). They have many advantages for this purpose, not the least of which is that they sample the rate at which individual stars form irrespective of the mass or luminosity of the host galaxy. We can therefore measure the total star formation over the entire range of galaxies. However, before we can do this, we must understand the biases in the selection of the stars that become GRBs and determine whether or not we can successfully allow for such selection effects.

The most probable bias is that GRBs occur only in low-metallicity galaxies and that we may therefore miss all of the star formation occurring in more evolved systems. In the collapsar models, GRBs are formed in single massive stars only if the metallicity is below $\sim 0.3\ Z_\odot$ (e.g., Woosley & Heger 2006). If such a bias is present, it could introduce a strong redshift dependence in the inferred star formation history if the average metallicity of the host galaxies is lower at high redshift.

The evidence of Figure 4 is somewhat confusing as regards this issue. In the first place, it shows that while most metallicities in GRB hosts could fall below $0.3\ Z_\odot$, at least one (GRB 000926, $Z = 0.7\ Z_\odot$; Savaglio et al. 2003) has a metallicity well above the critical value. Fynbo et al. (2006) suggest that this indicates that collapsars resulting from single massive stars are not the only progenitors of long GRBs, or that massive stars with $Z > 0.3\ Z_\odot$ can also produce long GRBs. It is also possible that this particular GRB formed in a lower metallicity region of the galaxy than that traversed by the sight line. However, if some of the measured metallicities are underestimates, this problem would become much more severe, and we would have to conclude that GRBs regularly form in high-metallicity environments. This issue clearly requires a much larger sample of very high quality spectra in order to be resolved.

Furthermore, if we do assume that GRBs are primarily formed in lower metallicity stars, then Figure 4 strongly suggests that metallicity bias will be extremely important in determining star formation rates. Most of the measured values lie just below the critical value and, presumably as their metallicity continues to increase, would drop from the sample. Since a large fraction of the star formation would occur in the higher metallicity objects, we would miss much of the activity. With precise metallicity measurements, we could make a detailed comparison with models of the star formation to see if the distribution was consistent and if the metallicity threshold was evident, but such a comparison is premature given the present quality of the data.

These data were obtained at the Gemini Observatory under Program ID GN-2006A-Q-14. We would like to thank Nestor Mirabal for helpful discussions and the Gemini North observing team for carrying out the observations. This work was supported by NSF grants AST04-07374 and AST06-07871, by NASA grants HST-GO-10616.02-A and Swift NN G05 G40G, and by *Spitzer* contract 1282161.

REFERENCES

Asplund, M., Grevesse, N., & Sauval, A. J. 2005, in ASP Conf. Ser. 336, Cosmic Abundances as Records of Stellar Evolution and Nucleosynthesis, ed. T. G. Barnes III & F. N. Bash (San Francisco: ASP), 25
Berger, E., Penprase, B. E., Cenko, S. B., Kulkarni, S. R., Fox, D. B., Steidel, C. C., & Reddy, N. A. 2006, ApJ, 642, 979
Chen, H.-W., Prochaska, J. X., Bloom, J. S., & Thompson, I. B. 2005, ApJ, 634, L25
Cowie, L. L., & Songaila, A. 1986, ARA&A, 24, 499
Fynbo, J. P. U., et al. 2006, A&A, 451, L47
Gehrels, N., et al. 2004, ApJ, 611, 1005
Hook, I. M., Jørgensen, I., Allington-Smith, J. R., Davies, R. L., Metcalfe, N., Murowinski, R. G., & Crampton, D. 2004, PASP, 116, 425
Jakobsson, P., et al. 2006a, A&A, 447, 897
———. 2006b, A&A, 460, L13
Kawai, N., et al. 2006, Nature, 440, 184
Krimm, H. A., et al. 2006, GCN Circ. 5096, http://gcn.gsfc.nasa.gov/gcn3/5096.gcn3
Lamb, D. Q., & Reichart, D. E. 2000, ApJ, 536, 1
Ledoux, C., Vreeswijk, P., & Ellison, S. 2005, GCN Circ. 3860, http://gcn.gsfc.nasa.gov/gcn3/3860.gcn3
Mirabal, N., & Halpern, J. 2006, GCN Circ. 5097, http://gcn.gsfc.nasa.gov/gcn3/5097.gcn3
Price, P. A., Cowie, L. L., Minezaki, T., Schmidt, B. P., Songaila, A., & Yoshii, Y. 2006a, ApJ, 645, 851
Price, P., et al. 2006b, GCN Circ. 5101, http://gcn.gsfc.nasa.gov/gcn3/5101.gcn3
———. 2006c, GCN Circ. 5104, http://gcn.gsfc.nasa.gov/gcn3/5104.gcn3
Prochaska, J. X. 2006, ApJ, 650, 272
Prochaska, J. X., Gawiser, E., Wolfe, A. M., Castro, S., & Djorgovski, S. G. 2003, ApJ, 595, L9
Savaglio, S. 2006, New J. Phys., 8, 195
Savaglio, S., Fall, S. M., & Fiore, F. 2003, ApJ, 585, 638
Songaila, A. 2004, AJ, 127, 2598
Songaila, A., & Cowie, L. L. 2002, AJ, 123, 2183
Stanek, K. Z., et al. 2003, ApJ, 591, L17
Starling, R. L. C., et al. 2005, A&A, 442, L21
Vreeswijk, P. M., et al. 2004, A&A, 419, 927
———. 2006, A&A, 447, 145
Watson, D., et al. 2006, ApJ, 652, 1011
Woosley, S. E. 1993, ApJ, 405, 273
Woosley, S. E., & Heger, A. 2006, ApJ, 637, 914